α-Synuclein pathology and mitochondrial dysfunction

van Zomeren, Koen Cornelis

Chapter 5

Modelling age-associated diseases using transgenic progerin expression

Zomeren, K.C. van[a], Hoes, M.F.[b], Tromp, J.[b], Boddeke, H.W.G.M[a], Meer, P. van der[b], Copray, J.C.V.M.[a]

a) Department of Neuroscience, section Medical Physiology, University Medical Center Groningen, Antonius Deusinglaan 1, 9713 AV, Groningen, The Netherlands
b) Department of Experimental Cardiology, University Medical Center Groningen, Antonius Deusinglaan 1, 9713 AV, Groningen, The Netherlands

Manuscript in preparation

Abstract

Human induced pluripotent stem cells (hiPSC) have transformed research since their discovery. The hiPSC technology enables detailed cellular studies on pathogenic processes in patient-derived somatic cell types that are specifically affected by the disease of the patient. However, due to the fact that these somatic cells are effectively rejuvenated during the iPSC reprogramming process, they have been considered less suitable for pathogenic studies on late-onset diseases, such as Parkinson's disease. We introduce a human in-vitro model to accelerate ageing of the iPSC-derived somatic cells using transgenic expression of progerin. Before application to our PD patient-derived DA neurons, we have chosen to test and implement our progerin-associated ageing model on embryonic stem cell differentiated cardiomyocytes. These cells can be easily differentiated, have a large soma easily accessible for microscopic analysis and display high mitochondrial activity allowing accurate evaluation of aging hallmarks. Differentiated cells that express progerin indeed displayed several hallmarks of ageing, including nuclear folding, chromosomal instability and mitochondrial dysfunction. Crucially, compared to earlier work by other groups, we can sustain progerin expression for up to at least 30 days, without apparent toxicity associated with the method for transgenic expression. Progerin-induced ageing on Parkinson's disease patient hiPSC-derived dopaminergic neurons resulted in neuronal cells with increased amounts of α-synuclein compared to control populations. This chapter presents the stem cell community with new tools to study ageing differentiated cells.

Introduction

Age-associated diseases pose an increasing burden on society and are often related to cellular senescence. Hallmarks of ageing are currently considered to be comprised of genomic instability, telomere attrition, epigenetic alterations, loss of proteostasis, deregulated nutrient

sensing, mitochondrial dysfunction, cellular senescence, stem cell exhaustion, and altered intercellular communication [1]. To properly model these processes in an ageing model for cell culture applications, scientists have come up with a number of ways to recapitulate parts of the ageing process. But, while most models mimic one hallmark of ageing, it remains difficult to tackle the multiple aspects of the ageing process. Cell models for late onset disorders, such as Parkinson's disease (PD), often use mitochondrial toxins [2-4], proteasome inhibitors [5], mimicking only part of the ageing process. Apart from this, cell models often consist of immortalized proliferating cells [6, 7], which are vastly different from somatic cells and make it difficult to model a senescent cell.

The use of human induced pluripotent stem cells (hiPSCs) and human embryonic stem cells (hESCs) has overcome part of this challenge since they can be differentiated into lineage-specific cells with a low mitotic index. However, reprogramming of somatic cells into iPSCs leads to their rejuvenation [8]. Telomere elongation, increased mitochondrial fitness and chromatin remodelling effectively restore iPSCs to an embryonic state that is beneficial for stemness. Thus, the reprogramming event also reverses several hallmarks of ageing making the resulting differentiated cells less suitable for modelling age-related disorders. Direct reprogramming of somatic cells is one way to overcome these challenges [9], but resulting cells are often unlike their somatic counterparts [10], and present epigenetic marks of the original cells after transdifferentiation [11].

An alternative method to overcome these challenges is using a mutated protein of Hutchinson-Gilford progeria syndrome (HGPS), a rare autosomal dominant disorder involving a splice variant of the *LMNA* gene [12]. The *LMNA* G608G (GGC>GGT) mutation in exon 11 activates a cryptic splice site leading to an aberrant form of the Lamin A/C protein, named progerin. Affected cells display a multiple hallmarks of ageing including nuclear deformation, DNA damage and mitochondrial

dysfunction [13]. Affected individuals usually die in the second decade of life from disorders usually associated with an aged population. Mental development is unaffected, and patients show no predisposition of neurodegeneration. This is due to a lack of Lamin A expression in the brain, where Lamin B and Lamin C are predominantly expressed [14].

Using progerin in a cell culture model for ageing has previously been introduced by Miller et al. [15], where it was elegantly shown that cells could be aged using progerin. However, procedural limitations prevented cells to be cultured for more than five days after progerin expression. Using modified RNA, cells were put under high transfection stress, resulting in major cell death even in the control group. To circumvent this problem, we decided to devise a lentiviral approach to expose cells to prolonged progerin expression.

This model has been extensively tested on hESC-derived cardiomyocytes (hESC-CMs), since *LMNA* laminopathies are usually associated with cardiac disease [16]. Furthermore, cardiac cells have high mitochondrial activity and are relatively easy to differentiate [17, 18]. By using the cardiac expression pattern during differentiation, transgenic progerin expression can be achieved using a conditional promoter. The ability to use cardiac cells at 30 days in vitro (DIV) compared to neurons at 60 DIV, allows for optimization of the method in a disease relevant cell type. After introduction and evaluation of the model in cardiomyocytes, we have used the same model on PD patient-derived neurons obtained via iPSC differentiation, to use it as a model for ageing.

In this chapter, we show that lentivirus-induced progerin expression in ESC-derived CMs leads to increased mitochondrial stress, nuclear deformation and an increase in double stranded break (DSB) formation of DNA. Additionally, we improved this ageing model for CMs by introducing a conditional promoter system for cardiac cell specific expression of progerin. Progerin expression in PD iPSC-derived neuronal cells leads to a typical accumulation of α-synuclein, a hallmark

of altered proteostasis not seen in control transduced PD iPSC-derived neuronal cells.

Materials and Methods

Culture of hESCs and hiPSCs

Human iPSCs were generated using a protocol described in chapter 3 of this thesis. Human HUES9 embryonic stem cells were provided by Harvard University HSCI iPS Core Facility.

Geltrex®-coated plates and Essential 8™ medium (Thermo Fisher Scientific) were used to maintain cells according to the manufacturer's instruction. Passaging of iPSCs was done using ReLeSR™ (Stemcell Technologies) according to the manufacturer's instruction, while passaging of ESCs was done using TrypLE™ Express (Thermo Fisher Scientific). All cells were maintained in a humidified incubator at 37°C with 5%CO_2. ESCs were used below passage 50, while iPSCs were used between passage 25 and 35.

Dopaminergic differentiation

Dopaminergic differentiation was achieved using a slightly adapted protocol from Kriks et al. [19], described in chapter 3 of this thesis. At day 20 of differentiation, cells were dissociated with Accutase (Sigma-Aldrich) and plated on Geltrex®-coated tissue culture treated plates. To purify cultures, cultures were exposed to glucose deprivation and lactate (5mM) supplementation (GDLS) at 26 days in vitro (DIV) after which neurons were maintained to 60 DIV. At 60DIV, transduction was performed after which cells were cultured for 30 DIV.

Cardiac differentiation

CMC differentiation of ESCs was achieved by dissociating HUES9 ESCs with 1x TrypLE Express for 4 minutes and plating them as single cells in Essential 8 medium containing 5 μM Y26732 (Selleck Chemicals). Once cultures reached 80% confluency, cells were washed with PBS and

differentiation was initiated (day 0) by culturing cells in RPMI1640 medium (Thermo Fisher Scientific) supplemented with 1x B27 minus insulin (Thermo Fisher Scientific) and 6 μM CHIR99021 (Cayman Chemical). At day 2, cells were washed with PBS and medium was refreshed with RPMI1640 supplemented with 1x B27 minus insulin and 2 μM Wnt-C59 (Tocris Bioscience). From day 4, medium was changed to CDM3 [17] medium and refreshed every other day as CM maintenance medium. This resulted in cultures with >90% spontaneously contracting CM at day 8-10. To further enrich these cultures, starting from day 12, differentiated CM were cultured in glucose-free RPMI1640-based (Thermo Fisher Scientific) CDM3 medium supplemented with 5 mM sodium DL-lactate (Sigma-Aldrich) for 6-10 days [20]. At 20DIV, medium was supplemented with triiodothyronine (Sigma-Aldrich) to enhance cardiomyocyte maturation and increase *MYH6* expression [21].

Vector construction

PCR amplification (Phusion High-Fidelity DNA Polymerase, Thermo Fisher Scientific) for AcGFP and AcGFP-progerin (a generous gift by Justine Miller) with overhangs for SpeI and KpnI was performed, and purified fragments were ligated in CloneJET vector (Thermo Fisher Scientific). Resulting CloneJET vectors and the pSin-EF2-Nanog-Pur vector (addgene plasmid 16578) were restricted using BcuI (SpeI, Thermo Fisher Scientific) and KpnI (Thermo Fisher Scientific), subsequently ligated using T4 ligase (Thermo Fisher Scientific) after which the product was transformed in DH5α competent cells. Colony PCR screening was performed to select positive colonies, which were checked by restriction analysis. Correct plasmids were sent for sequencing and transfected in HEK293T to validate expression.

A conditional vector for AcGFP and AcGFP-progerin expression was created at Oxford Genetics. To achieve expression, inserts were placed under control of the α-MHC promoter, which is flanked by an EF1a-PuroR cassette to allow puromycin selection of transduced cells.

The cassette is flanked by a Woodchuck Hepatitis Virus (WHP) Posttranscriptional Regulatory Element (WPRE) for stable expression of the transgenes.

Viral transduction

Viral transduction was using a slightly modified protocol by Trono et al. (Production and titration of lentiviral vectors) achieved by transfecting a T75 of HEK-293T cells when cells were 70-80% confluent. A mixture containing 900 µl OPTIMEM (Thermo Fisher Scientific) 9 µg viral vector, 3 µg pMD2-VSV-G and 7.5 µg pCMV-D8.91, was supplemented with 45 µl FUGENE HD (Lonza) and incubated for 15 min at room temperature (RT) to generate transfection complexes. The next day medium was changed with 20 ml RPMI 1640 (Thermo Fisher Scientific) and viral particles were harvested between 36 and 48 h. Viral supernatant was collected and sterilized using a 0.45 µm filter (Nalgene), subsequently mixed with CDM3 in a 1:1 ratio for AcGFP-progerin, and a 1:4 ratio for AcGFP. The resulting mixture was supplemented with polybrene (8 µg/ml). HUES9 derived CMs were dissociated using 1x TrypLE Express, spun down at 200g, resuspended in low volume and added to the viral mixture. The next day cells were washed with dPBS, and medium was changed to CDM3.

Transducing HUES9 ES cells with the conditional promoter system was achieved using a similar protocol as described above, with minor modifications. HEK293T cells were transfected with the pSF-OxG-Lenti-aMHC-AcGFP-(Progerin)-Puro-WPRE vector, constructed by Oxford Genetics custom cloning and viral supernatant was collected in E8 medium w/o supplement. After transduction, HUES9 cells were cultured with 50µg puromycin to obtain clones with similar integration profiles. Resulting cultures were single cell sorted using a flow cytometer and expanded to be analysed using genomic DNA qPCR.

Immunocytochemistry

Borosilicate glass coverslips containing cells were fixed in paraformaldehyde 4% for 15 min at room temperature and stored at 4°C. Permeabilization and blocking were done in PBS containing 0.1% Triton, 1% BSA and 5% normal goat serum for ~60 min at RT. Primary antibody incubation was done overnight at 6°C, followed by three PBS washes (5 min each), after which a fluorescent conjugated secondary antibody and Hoechst 33258 (Sigma-Aldrich, 14530) were added. Mowiol® 4-88 (Sigma-Aldrich) was used as mounting medium to attach the coverslips to glass slides. Samples were stored at 4°C until further analysis. Primary antibodies used were monoclonal anti-α-actinin IgG1 (1:100; A7811, Sigma-Aldrich), polyclonal anti-cardiac troponin T IgG (1:100; ab45932, Abcam) polyclonal anti-TOM20 IgG (1:250; sc-11415, Santa Cruz Biotech), monoclonal Anti-phospho-Histone H2A.X (Ser139) (1:100, clone JBW301, Millipore).

Imaging

Phase contrast imaging was performed on a Leica AF-6000 microscope, using a 20x objective (PL FLUOTAR 20x/NA 0.4, Dry).

Confocal images were acquired using a Leica SP8 confocal microscope, equipped with an HC PLAPO CS2 63x oil lens, with NA 1.4. Epifluorescence images were acquired using a Leica AF-6000 fluorescent microscope, using a PL FLUOTAR 20x/NA 0.4, Dry lens.

CellROX™ assay

To perform CellROX™ (Thermo Fisher Scientific) assays, cells were plated and transduced in a Geltrex®-coated 96 well plate. After two weeks of transgenic expression, medium was changed to CDM3 without phenol red 2 hours prior to measurement. For measurement, 25µl of CDM3 without phenol red supplemented with 5µM CellROX™ orange and 10mM HEPES was added to the wells. Fluorescent signal (Ex/Em: 540/570) was measured every minute for 2h by a SYNERGY H1 plate

reader (BIOTEK), and the area under curve (AUC) was calculated from the resulting data. Experiments were performed in n=5 independent differentiations.

Genomic DNA qPCR

Single cell sorted HUES9 clones were expanded for two passages, and genomic DNA was extracted using a QIAamp DNA Mini Kit (QIAGEN). In order to find the right conditions for qPCR on gDNA, primer test experiments were performed for the GAPDH (Fw: GGCTCCCACCTTTCTCATCC, Rev: CTCCCCACATCACCCCTCTA) and AcGFP (Fw: CGAGCTGAATGGCGATGTGA, Rev: CCGGTGGTGCAGATGAACT) primer using different primer concentrations, and different input of genomic DNA. Using this data, we determined the optimal concentration to compare the amount of AcGFP integration between clones. To determine the amount of integration samples were mixed with primers (5nM) and IQ SYBR Green (170-8885, BioRad). Samples were run on a Biorad C1000 Touch thermal cycler and analyzed with Biorad CFX manager™ software.

Statistical analysis

All statistical tests were performed using Prism 7.0. Statistical significance was determined using one-way ANOVA followed by Tukey post hoc test. A p value < 0.05 was considered significant. With biological replicates lower than n=3 no significance was indicated.

Results

To introduce viral expression of AcGFP and AcGFP-progerin, several vectors were used. To introduce progerin expression in initial experiments, a vector with a strong promoter and easy vector design was chosen to directly transduce differentiated cardiomyocytes. After initial findings a second expression system was introduced, using conditional promoter driven expression of AcGFP and AcGFP-progerin. This design

enables the study of clonal lines, allowing more stable expression between control and progerin expressing lines and takes away the need for directly transducing differentiated cultures.

HUES9 CMs can be successfully transduced by an AcGFP-progerin viral vector

Construction of the viral vector was based on the pSinEF2 vector with AcGFP or AcGFP-progerin placed under expression of the EF1a promoter (Figure 1A). Testing of the vector in HEK293T cells showed a robust expression of the viral vector (Figure 1B). Additionally, CMs were transduced successfully (Figure 1C). Transgenic AcGFP-progerin expression showed progerin localisation around the nuclear lamina (Figure 1C).

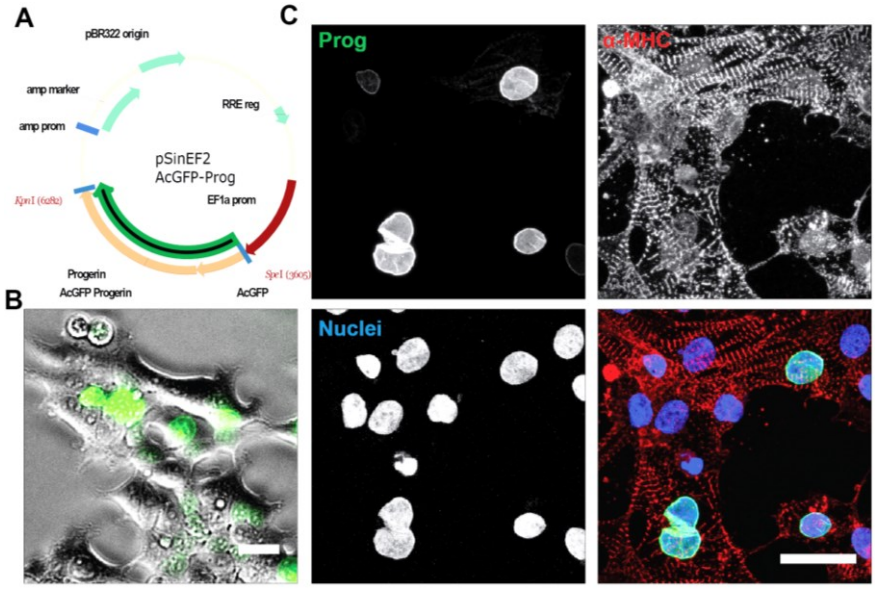

Figure 1. AcGFP-progerin can be successfully expressed in CMs. (A) *Vector map of the pSinEF2-AcGFP-progerin viral vector. AcGFP-progerin is placed under control of the EF1-α promoter.* ***(B)*** *HEK293T cells expressing the AcGFP-progerin vector.* ***(C)*** *CMC cultures successfully transduced by AcGFP-Progerin. Striated α-actinin structures (red), AcGFP-progerin and Hoechst (blue) are shown at 40DIV. All bars represent 25 μm.*

Progerin expression leads to oxidative stress

AcGFP-progerin-expressing CMs produced significantly more ROS compared to AcGFP expressing and control CMs. Figure 2A displays fluorescent images of measured CMs. The amount of transduced cells was similar between AcGFP and AcGFP-progerin. Expression of AcGFP-progerin showed a significant increase (19.4%) in ROS production compared to control ($p<0.0001$) and to AcGFP-expressing CMs ($p<0.0001$) (Figure 2B).

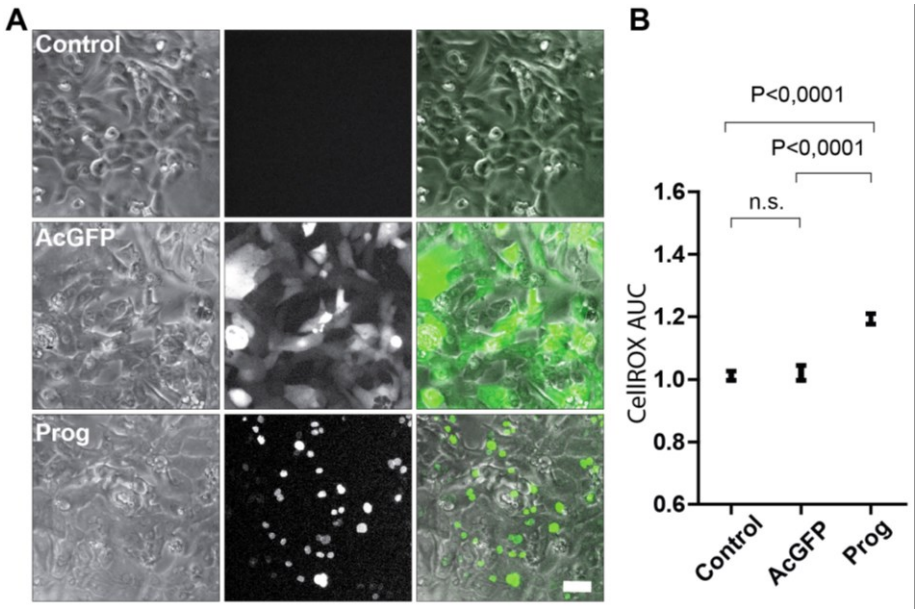

Figure 2. AcGFP-progerin expression leads to an increase in ROS production. (A) *Transduction with AcGFP and AcGFP-progerin vectors. AcGFP-progerin co-localizes with the nuclear membrane, while AcGFP is expressed diffusely in the cytoplasm. Scalebar represents 25 µm.* ***(B)*** *ROS production is higher in AcGFP-progerin expressing cells (19.4% increase), while it remains similar between control and AcGFP (2.1%, n.s.). All data were produced with n=5 biological replicates.*

Progerin expression leads to an increase in double stranded breaks

Double stranded break (DSB) incidence was quantified by counting γH2AX-positive foci-containing cells, where only cells with 2 or

more γH2AX foci are considered positive and included, as sporadic incidence of DSBs is a normal consequence of mammalian cell culture. AcGFP-progerin expressing cells were frequently observed to have more than 20 of such foci. Figure 3A shows an example of a quantified image, with a high incidence of DSBs in AcGFP-progerin-expressing CMs compared to control and AcGFP-expressing CMs. Transduction efficiencies for AcGFP and AcGFP-progerin were 55.0% and 53.3% respectively (Figure 3B). Incidence of γH2AX foci in control cells was 10.5%, while incidence in the cells in the AcGFP images was 12.1% and 12.35%, respectively for AcGFP-negative and AcGFP-positive foci. Interestingly, AcGFP-progerin images showed an increase in cells with foci for both AcGFP-progerin-positive (53.3%) and -negative cells (20.3%).

Transgene expression in a conditional CMC promoter

To validate our findings using direct transduction of CMs, we have chosen to develop a model that allows conditional expression of AcGFP-progerin; the set-up of the viral vector is shown in figure 4a. Figure 4B displays the expression of the vector in mixed cultures, after culture for 34DIV. At this time point, CMs are active and contract as evidenced by analysis with difference tracker (Figure 4C). The highlighted section at 7.75s is an overlay with the moving pixels in the image, indicating the contraction of cells in red. To select individual clones for further analysis, we decided to screen integration sites using a qPCR assay on genomic DNA. For this purpose, previously puromycin-selected transduced HUES9 cells were single cell sorted and cultured after which gDNA was extracted. Optimal primer conditions and gDNA input were determined and AcGFP integration was normalized to genomic GAPDH content. From our data we selected two AcGFP and two AcGFP-progerin clones which had closely matching integration of the viral vector (Figure 4D).

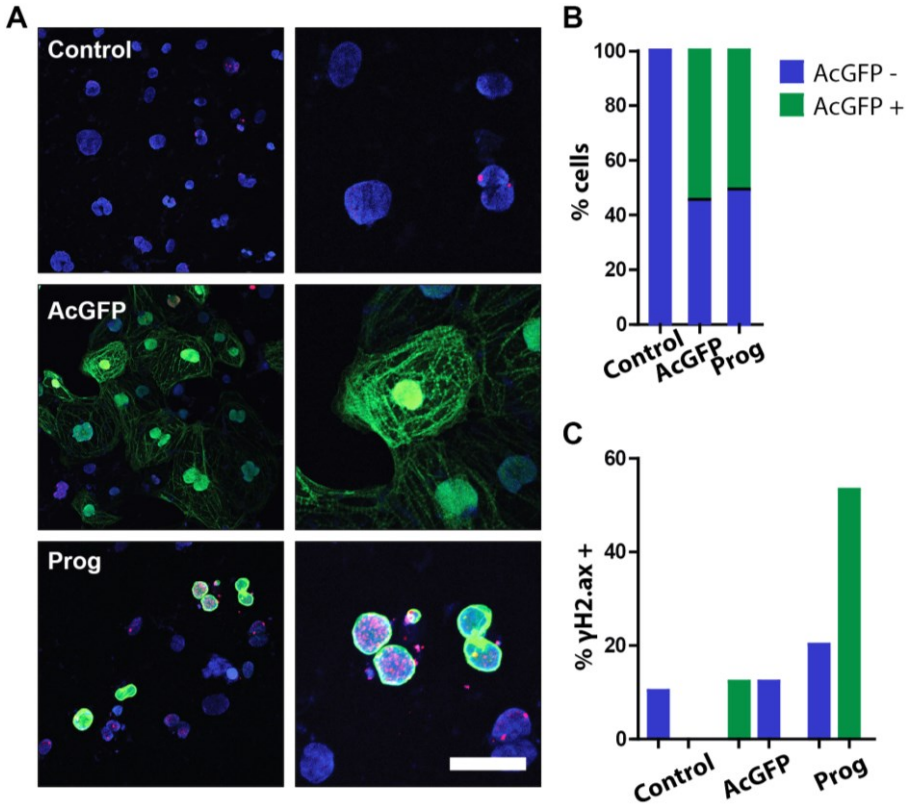

Figure 3. AcGFP-progerin expression leads to increased DSB incidence. (A) *Corresponding images of control and AcGFP (green) and AcGFP-progerin (green) transduced cells. A γH2AX staining is presented in the red channel, and Hoechst is depicted in blue. Scalebar represents 25 µm.* ***(B)*** *Transduction efficiency in CMs is presented as AcGFP positive (green) and negative cells (blue).* ***(C)*** *Occurrence of DSBs as assessed by the percentage of cells containing 2 or more γH2AX positive foci is more frequent in AcGFP-progerin-transduced cells compared to control and AcGFP-transduced cells. Non-transduced cells present in the progerin condition also display an increase in γH2AX foci. Data was produced with n=2 biological replicates.*

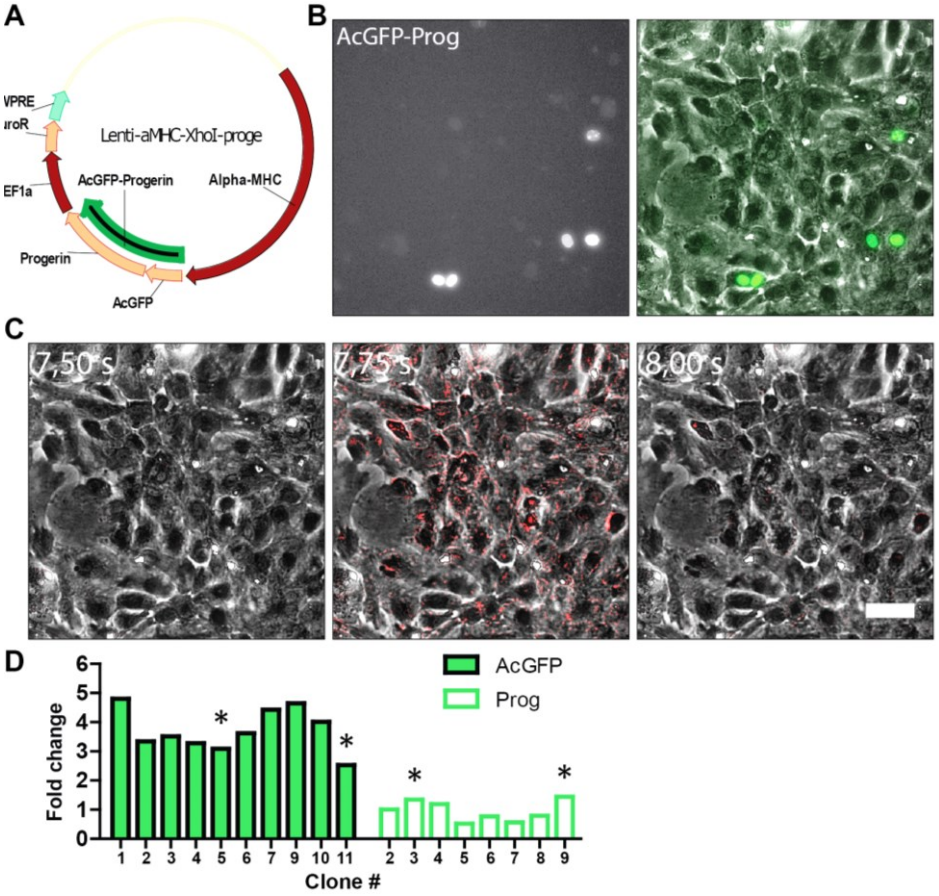

Figure 4. AcGFP-progerin can be expressed under the αMHC promoter in CMs. ***(A)*** *Viral vector map of pSF-OxG-Lenti-aMHC-AcGFP-(Progerin)-Puro-WPRE. AcGFP-progerin is placed under control of the α-MHC promoter, and flanked by an EF1α-PuroR cassette.* ***(B)*** *CMC cultures successfully express AcGFP-progerin (green) under the α-MHC promoter at 30DIV. The observed heterogeneity is the result of culturing a non-clonal cell population.* ***(C)*** *CMC cultures are functional at 30DIV, as evidenced by contraction highlighted by difference tracker. Bar represents 25 µm.* ***(D)*** *AcGFP integration normalized to GAPDH for AcGFP and AcGFP-progerin transduced HUES9 ESCs. Selected clones are denoted by an asterisk*.*

AcGFP-progerin can be expressed under the conditional α-MHC promoter in CMs

Figure 5A demonstrates the expression of AcGFP-progerin (white) in a cardiomyocytes culture. Alpha-actinin (green) staining shows the sarcomeric structure of CMs, with co-localizing expression of troponin-T (red). Expression of LAMINA/C is illustrated in Figure 5B, and shows co-localisation with AcGFP-progerin, indicating correct nuclear localisation. A staining with the gap junction protein Connexin-43 (Cx43) highlights the connections between adjacent cells. A mitochondrial TOMM20 (red) staining in Figure 5C displays no apparent defects in mitochondrial integrity in AcGFP-progerin (green) expressing cells. Although γH2AX (white) positive foci were occasionally observed in AcGFP-progerin expressing cells, their frequency was low.

Neuronal AcGFP-progerin expression results in increased levels of α-synuclein

To use our progerin expression model system in neuronal cells, we used the earlier described pSinEF2-AcGFP-progerin vector for direct transduction of differentiated cultures. Transgenic expression was achieved at 60DIV and maintained for 30DIV in purified neuronal cultures. This resulted in a marked increase of the amount of α-synuclein fluorescence when compared to AcGFP control. Expression of AcGFP-progerin in differentiated PD patient iPSCs led to increased levels of α-synuclein in these cells as assessed by confocal microscopy (Figure 6). Figure 6A shows expression of the AcGFP control vector, combined with TH (red), α-synuclein (yellow) and Hoechst (blue). Figure 6B shows expression of the AcGFP-progerin vector, combined with TH (red), α-synuclein (yellow) and Hoechst (blue).

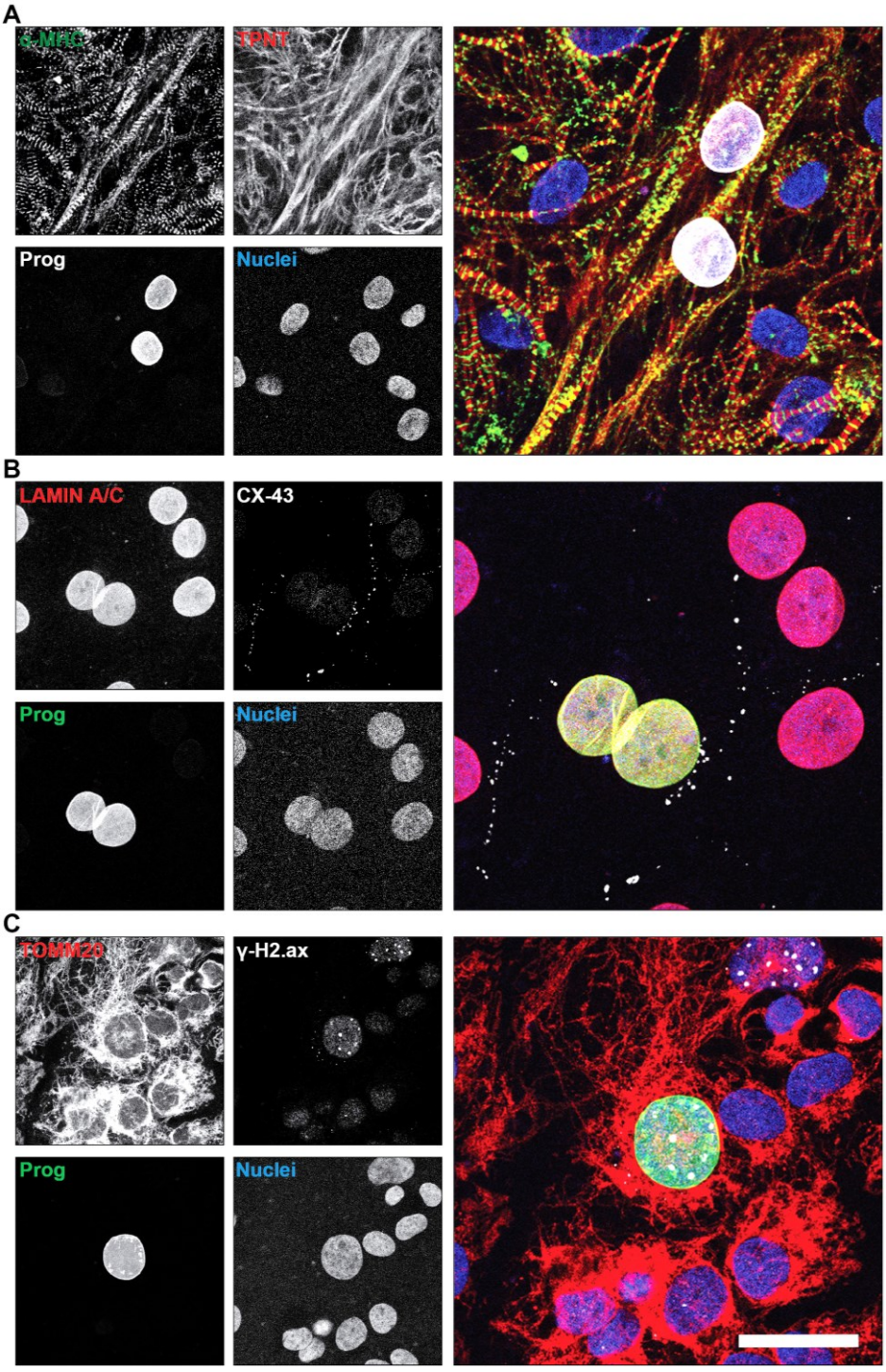
A
c-MHC
TPNT
Prog
Nuclei
B
LAMIN A/C
CX-43
Prog
Nuclei
C
TOMM20
γ-H2.ax
Prog
Nuclei

Figure 5. CMs confocal microscopy highlights functional characteristic. (A) *CMs express striated α-actinin (red) structures and a structural distribution of troponin-T (green). AcGFP-progerin and Hoechst are presented in white and blue respectively.* ***(B)*** *CMs express laminA/C, which shows overlap with the AcGFP-progerin signal (green). Connexin43 staining highlights the gap junctions between CMs, and Hoechst is depicted in blue.* ***(C)*** *CMs show no abnormalities in mitochondrial networks as evidenced by TOMM20 (red). γH2AX foci (white) were present, but not frequently observed. AcGFP-progerin and Hoechst are presented in white and blue respectively. Bar represents 25 μm.*

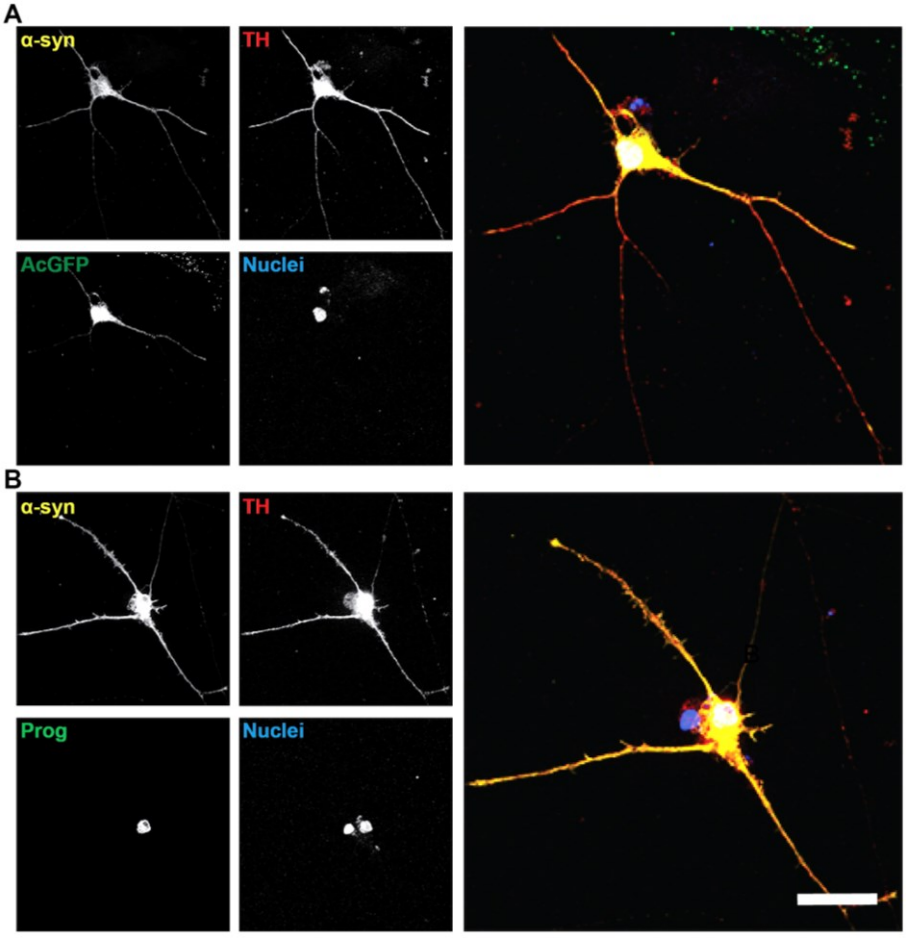

Figure 6. DA neurons expressing AcGFP-progerin have increased levels of α-synuclein.

(A) *PD4 iPSC-derived DA neuron expressing AcGFP (green), stained for TH (red), α-synuclein (yellow) and Hoechst (blue).* ***(B)*** *PD4 iPSC-derived DA neuron expressing AcGFP-progerin (green), stained for TH (red), α-synuclein (yellow) and Hoechst (blue). Comparison of α-synuclein-associated fluorescence shows a marked increase between AcGFP and AcGFP-progerin transduced iPSC-derived DA neurons. Bar represents 25 µm.*

Discussion and conclusion

In this chapter, we successfully recapitulated ageing hallmarks by inducing overexpression of progerin in both neuronal and cardiac cells. The lentiviral approach allowed us to induce transgenic expression of progerin for prolonged periods of time (>30DIV). Our model recapitulates hallmarks of ageing which could not be produced by the approach of Miller et al. [15]. However, a downside of our viral approach is the uncontrolled integration of the viral vector, which can interfere with gene integrity and expression. This is solved by using a large population of post-mitotic cells, that will create a heterogeneous profile of viral integrates, effectively diluting any negative effects of viral integration. In our conditional promoter approach, however, viral integration might produce a problem since we are using clonal cells. To prevent harmful viral integration in these models, a non-restrictive linear amplification-mediated PCR should be performed to identify integration sites [22].

The occurrence of increased oxidative stress and the increase in γH2AX-positive foci indicates that our model captures both genomic instability and mitochondrial dysfunction. Interestingly, mitochondrial ROS production is significant but not as pronounced compared to other model systems. Over two-fold increases in ROS generation are common when exposing cells to mitochondrial toxins like rotenone or paraquat, but our approach reports an increase of only 19.4%. In this light, our model recaptures more physiological levels of ROS increase that might lead to cellular damage over time. Mitochondrial abnormalities were not apparent

in confocal microscopy and it remains to be investigated whether the mitochondrial membrane potential is affected. The ability to induce long-term mitochondrial toxicity by nuclear stress provides an indirect mechanism for manipulating mitochondrial function and so provides a relevant tool for studying mitochondrial function in ageing. Mitochondrial function will be further analysed in mitochondrial respiration and glycolysis assays using the Agilent Seahorse XF Technology, as oxidative phosphorylation has been proposed to be progressively impaired during ageing [23].

The increase in γH2AX was an expected effect in progerin pathology. The large number of foci present in some of the cells point to extensive nuclear instability. Surprisingly, non-transduced cells in the progerin-transduced cultures also presented a higher number of foci indicating that an indirect effect may contribute to nuclear pathology. The overall increase in ROS production in these cultures might increase the indirect formation of DSBs in non-transduced cells [24] or might be the result of senescent paracrine signalling by progerin transduced cells [25].

In human iPSC derived DA neurons, progerin-induced ageing in resulted in higher levels of α-synuclein compared to controls. The underlying cause for this increase remains to be investigated, but might stem from altered proteostasis in these neurons. Another option is the induction of aggregation by increased oxidative stress, which has a direct effect on α-synuclein oligomerization [26, 27]. It should be noted that while progerin can be used as an ageing model in these cells, neurons do not express Lamin-A or progerin in vivo *[28]*. Progerin induced ageing might therefore not be as physiologically relevant to the brain as it is to other organs, i.e. cardiomyocytes. It does, however, represent a model that recaptures multiple hallmarks of ageing.

In summary, we present an alternative method to age cells, and show that functional CMs generated from HUES9 ESCs exposed to this method exhibit several characteristics of aging. Future experiments will

rely on a conditional promoter approach, and will validate earlier findings done in directly transduced CMs.

References

1. Lopez-Otin C, Blasco MA, Partridge L et al. The hallmarks of aging. **Cell**. 2013;153:1194-1217.
2. Gen W, Tani M, Takeshita J et al. Mechanisms of Ca2+ overload induced by extracellular H2O2 in quiescent isolated rat cardiomyocytes. **Basic research in cardiology**. 2001;96:623-629.
3. Ryan SD, Dolatabadi N, Chan SF et al. Isogenic human iPSC Parkinson's model shows nitrosative stress-induced dysfunction in MEF2-PGC1alpha transcription. **Cell**. 2013;155:1351-1364.
4. Zhang HY, McPherson BC, Liu H et al. H(2)O(2) opens mitochondrial K(ATP) channels and inhibits GABA receptors via protein kinase C-epsilon in cardiomyocytes. **American journal of physiology Heart and circulatory physiology**. 2002;282:H1395-1403.
5. Rideout HJ, Larsen KE, Sulzer D et al. Proteasomal inhibition leads to formation of ubiquitin/alpha-synuclein-immunoreactive inclusions in PC12 cells. **Journal of neurochemistry**. 2001;78:899-908.
6. White SM, Constantin PE, Claycomb WC. Cardiac physiology at the cellular level: use of cultured HL-1 cardiomyocytes for studies of cardiac muscle cell structure and function. **American journal of physiology Heart and circulatory physiology**. 2004;286:H823-829.
7. Xie HR, Hu LS, Li GY. SH-SY5Y human neuroblastoma cell line: in vitro cell model of dopaminergic neurons in Parkinson's disease. **Chinese medical journal**. 2010;123:1086-1092.
8. Lapasset L, Milhavet O, Prieur A et al. Rejuvenating senescent and centenarian human cells by reprogramming through the pluripotent state. **Genes & development**. 2011;25:2248-2253.
9. Mertens J, Paquola AC, Ku M et al. Directly Reprogrammed Human Neurons Retain Aging-Associated Transcriptomic Signatures and Reveal Age-Related Nucleocytoplasmic Defects. **Cell stem cell**. 2015;17:705-718.
10. Hanna JH, Saha K, Jaenisch R. Pluripotency and cellular reprogramming: facts, hypotheses, unresolved issues. **Cell**. 2010;143:508-525.

11. Zhou Q, Melton DA. Extreme makeover: converting one cell into another. **Cell stem cell**. 2008;3:382-388.
12. Moulson CL, Fong LG, Gardner JM et al. Increased progerin expression associated with unusual LMNA mutations causes severe progeroid syndromes. **Human mutation**. 2007;28:882-889.
13. Cao K, Blair CD, Faddah DA et al. Progerin and telomere dysfunction collaborate to trigger cellular senescence in normal human fibroblasts. **The Journal of clinical investigation**. 2011;121:2833-2844.
14. Jung HJ, Coffinier C, Choe Y et al. Regulation of prelamin A but not lamin C by miR-9, a brain-specific microRNA. **Proceedings of the National Academy of Sciences of the United States of America**. 2012;109:E423-431.
15. Miller JD, Ganat YM, Kishinevsky S et al. Human iPSC-based modeling of late-onset disease via progerin-induced aging. **Cell stem cell**. 2013;13:691-705.
16. van der Kooi AJ, Bonne G, Eymard B et al. Lamin A/C mutations with lipodystrophy, cardiac abnormalities, and muscular dystrophy. **Neurology**. 2002;59:620-623.
17. Burridge PW, Holmstrom A, Wu JC. Chemically Defined Culture and Cardiomyocyte Differentiation of Human Pluripotent Stem Cells. **Current protocols in human genetics**. 2015;87:21 23 21-15.
18. Lian X, Hsiao C, Wilson G et al. Robust cardiomyocyte differentiation from human pluripotent stem cells via temporal modulation of canonical Wnt signaling. **Proceedings of the National Academy of Sciences of the United States of America**. 2012;109:E1848-1857.
19. Kriks S, Shim JW, Piao J et al. Dopamine neurons derived from human ES cells efficiently engraft in animal models of Parkinson's disease. **Nature**. 2011;480:547-551.
20. Tohyama S, Hattori F, Sano M et al. Distinct metabolic flow enables large-scale purification of mouse and human pluripotent stem cell-derived cardiomyocytes. **Cell stem cell**. 2013;12:127-137.
21. Lee YK, Ng KM, Chan YC et al. Triiodothyronine promotes cardiac differentiation and maturation of embryonic stem cells via the classical genomic pathway. **Molecular endocrinology**. 2010;24:1728-1736.
22. Gabriel R, Kutschera I, Bartholomae CC et al. Linear amplification mediated PCR--localization of genetic elements and characterization of unknown flanking DNA. **Journal of visualized experiments : JoVE**. 2014:e51543.
23. Lesnefsky EJ, Hoppel CL. Oxidative phosphorylation and aging. **Ageing research reviews**. 2006;5:402-433.

24. Vilenchik MM, Knudson AG. Endogenous DNA double-strand breaks: production, fidelity of repair, and induction of cancer. **Proceedings of the National Academy of Sciences of the United States of America**. 2003;100:12871-12876.
25. van Deursen JM. The role of senescent cells in ageing. **Nature**. 2014;509:439-446.
26. Paxinou E, Chen Q, Weisse M et al. Induction of alpha-synuclein aggregation by intracellular nitrative insult. **The Journal of neuroscience : the official journal of the Society for Neuroscience**. 2001;21:8053-8061.
27. Esteves AR, Arduino DM, Swerdlow RH et al. Oxidative stress involvement in alpha-synuclein oligomerization in Parkinson's disease cybrids. **Antioxidants & redox signaling**. 2009;11:439-448.
28. Nissan X, Blondel S, Navarro C et al. Unique preservation of neural cells in Hutchinson- Gilford progeria syndrome is due to the expression of the neural-specific miR-9 microRNA. **Cell reports**. 2012;2:1-9.